

## Article

# Efficient Management of Fast Charging Systems Based on a Real-Time Monitoring System

Do-Hyun Kim , Min-Soo Kim , Kandasamy Prabakar \* and Hee-Je Kim \* 

Department of Electrical Engineering, Pusan National University, Pusan 46241, Korea; kdh8486@naver.com (D.-H.K.); rlaalstn5122@naver.com (M.-S.K.)

\* Correspondence: kprabakar@gmail.com (K.P.); heeje@pusan.ac.kr (H.-J.K.); Tel.: +82-51-510-7334 (K.P.); +82-51-510-2364 (H.-J.K.)

**Abstract:** Fast charging technology is attracting attention due to the increase in the use of batteries such as EV (Electric Vehicle), LEV (Light Electric Vehicle) and ESSs (Energy Storage Systems). Fast charging of the battery has problems such as fire, heat, and performance degradation of the battery. In the case of fast charging, a large current is applied to the battery to charge it. For this reason, information of battery voltage, battery current and temperature is important when charging a battery. Excessive current, overvoltage, and overheating beyond the standard value can cause deterioration of battery performance and a direct cause of fire. Therefore, the condition of the battery must be operated in the condition that meets the battery standard. To overcome these problems, we are trying to solve problems such as battery overheating and accidents by applying real-time monitoring technology, User Mode and Auto Control Mode. In this paper, we propose a real-time monitoring system based on the PHPOC Wi-Fi Shield. It operates to efficiently manage the charger and battery status based on real-time data, and is verified through real-time monitoring of the proposed system.

**Keywords:** LEV (Light Electric Vehicle); ESS (Energy Storage System); monitoring system; fast charging technology



**Citation:** Kim, D.-H.; Kim, M.-S.; Prabakar, K.; Kim, H.-J. Efficient Management of Fast Charging Systems Based on a Real-Time Monitoring System. *Electronics* **2022**, *11*, 520. <https://doi.org/10.3390/electronics11040520>

Academic Editors: Srikanta Patnaik, Shengqing Li and Jianqi Li

Received: 17 January 2022

Accepted: 8 February 2022

Published: 10 February 2022

**Publisher's Note:** MDPI stays neutral with regard to jurisdictional claims in published maps and institutional affiliations.



**Copyright:** © 2022 by the authors. Licensee MDPI, Basel, Switzerland. This article is an open access article distributed under the terms and conditions of the Creative Commons Attribution (CC BY) license (<https://creativecommons.org/licenses/by/4.0/>).

## 1. Introduction

Globally, the problem of environmental pollution and air pollution is a key issue. Vehicles using fossil fuels are a major cause of environmental pollution due to exhaust gas. Recently, many battery-based technologies, such as ESS, EV, and LEV have been introduced in accordance with the growth of the battery market and environmental pollution problems. The battery market share is growing day by day, and exhaust-gas-free EVs and LEVs will solve the problem of air pollution. In addition, compared to a general vehicle, it has the advantage of less maintenance and less noise; however, fires frequently occur in many lithium-ion battery-based ESS, EV, and LEV operating worldwide. The risk is high, especially for topologies that use high currents, such as fast charging. A lot of research on charging technology and charging efficiency is in progress. On the other hand, studies on charging monitoring and management are still rare compared to charging-related studies [1,2].

In the case of fast charging technology, the C-rate of the battery is higher than that of a general charging system. Therefore, as the charging current increases, the amount of power increases. High charging current causes battery heat, overcharge, and over-discharge. In order to efficiently manage the battery, it is necessary to check the charging current and voltage status of the battery in real-time. In addition, depending on the temperature condition of the battery, an appropriate current control system can solve the heat generation problem. In the case of a large ESS system, a temperature control system for temperature heating is applied. However, systems such as LEVs often do not have systems that can control temperature. Failure to properly control the temperature can be dangerous enough

to cause a fire in the worst case. Lithium-ion batteries are expensive, and if a fire breaks out, the charging system and LEV system would fail. If the temperature can be checked in real-time, charging can be made safely depending on the battery condition. By quickly providing the user with battery conditions, accidents such as fires and explosions that occur during charging can be prevented [3–5].

LLC resonant converters are used in various industries and applications because they can perform power conversion with high density and high efficiency [6,7]. The resonance converter may adjust the output voltage by controlling the frequency by changing the voltage gain according to the switching frequency. Fast charging systems generally use CC (Constant Current) and CV (Constant Voltage). CC is a method of charging using a constant current, and in fast charging, a high current is charged compared to a general charger. On the other hand, CV is a constant voltage charging method that charges until a certain voltage is reached. CC–CV (Constant Current – Constant Voltage) starts with CC at the initial stage of charging and is charged in a CV state when it reaches a state of charge (SOC) of 70 to 80% [8–10]. In the initial state, charging proceeds quickly in the current control state. The battery is fully charged with a predetermined voltage through the voltage controller.

In [11], internet of things (IoT) technology was applied to achieve efficient communication between the interdependent components of an EV charger. Data are collected, stored, analyzed, and shared with IoT devices from smartphones [12]. In the case of a user-friendly IoT system such as [13], the user can easily check the battery status through monitoring. The user can obtain information through a smartphone and usefully check the battery charge status; however, it does not take temperature into account, so the charging rate may affect the battery. In the case of EV and LEV chargers as in [14,15], the user cannot check the state of charge of the battery. Therefore, it is not easy for the user to efficiently manage the battery. In addition, most studies are focused on efficiency rather than user-friendly research-based on IoT. Power conversion efficiency is also an important factor, but research is needed to enable users to efficiently manage battery status information and efficiency.

This study proposes a fast charger using an LLC resonant converter. In addition, a monitoring system is proposed to efficiently manage the temperature, charging voltage, and current of the battery in real-time. Fast charging power operates in a soft-switching state in the DC/DC stage. We propose efficient management of fast charging systems based on a real-time monitoring system. The rest of this paper is organized in seven sections. After introduction, the system overview is demonstrated in Section 2. The proposed controller structure is described in Section 3. Additionally, the results and discussion are verified in Section 4. We summarize the results in Section 5.

## 2. System Overview

The proposed management of the fast charging system is depicted in Figure 1. The charging system consists of AC/DC Rectifier, Full bridge LLC resonant converter and battery. AC power is used, and AC power is converted into DC power through AC/DC Rectifier. LLC resonant converter modulates the frequency from DSP (TMS320F28335, Texas Instruments, Dallas, TX, USA) through Pulse Frequency Modulation (PFM) control. In the case of a resonant converter, unlike a PWM converter, the output can be controlled through frequency. The resonant converter has the highest efficiency at the resonant frequency. Arduino measures temperature, input current, input voltage, output voltage and output current through ADC. Arduino is connected to a PHPOC Wi-Fi Shield to measure and calculate output voltage, output current, temperature, and power through a web server. The measured data is transmitted to the web server. Data from the web server can be checked through the smartphone app. The user can check the data in real-time, and the control current value is determined according to the temperature. The control current command calculated considering the temperature is transmitted to the TMS320F28335 and controlled [16].

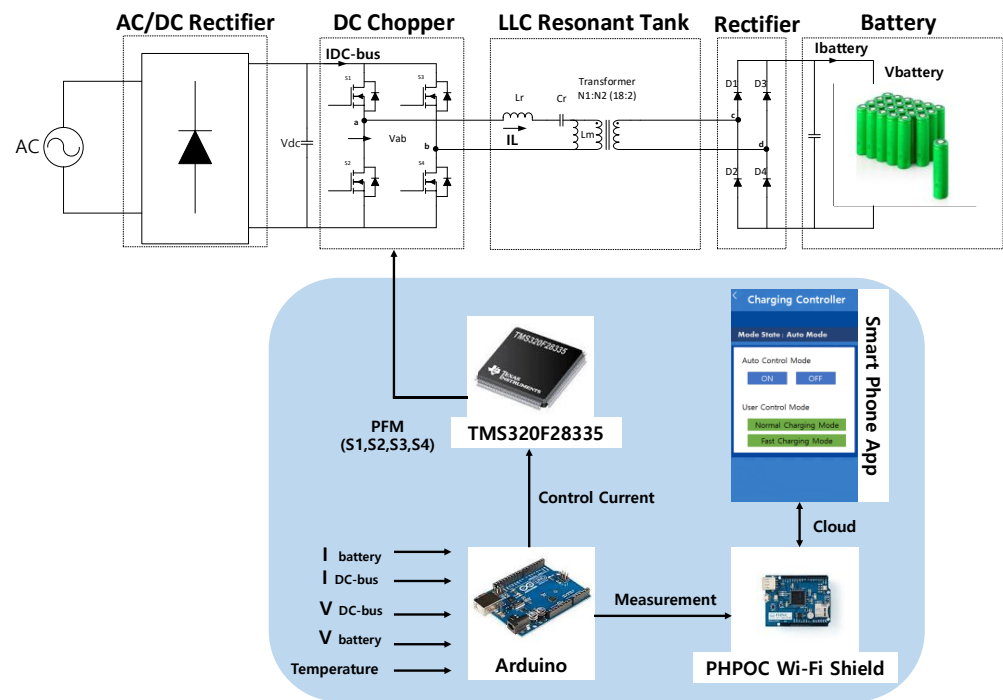


Figure 1. Proposed Real-time monitoring system overview.

2.1. IoT-Based Controller

The main goal of IoT-based is to propose a system to remotely adjust the LEV charging current and monitor the charging status according to the real-time status. The design of a smartphone application and a real-time monitoring system is presented in this section. Users can check the monitoring of various charger variables in real-time. The proposed structure of the monitoring system includes voltage, current and temperature sensor, Arduino, PHPOC Wi-Fi shield, as shown in Figure 1. A user-friendly application has been developed using App Inventor2 from Google. Table 1 shows the specification of the employed the Wi-Fi module [17]. The control process is implemented by the DSP board. Arduino converts analog data into digital data through an A/D conversion process. In the case of the Wi-Fi module, it is in charge of communication work necessary to deliver digital data to the cloud. User input values are communicated to the web server, which can be used as input to the charge controller. The input current value used is transmitted to the DSP board through the Arduino.

Table 1. Specification of PHPOC Wi-Fi Shield.

	Core	Cortes-M4 168MHz
Processor	Flash	System-512K Bytes, User-512K Bytes
	SRAM	192K Bytes
	Interface	IEEE802.11b/g Wireless LAN (require RalinkRT3070/5370 chipset Wireless LAN Adapter)
Wireless LAN	Mode	Ad-hoc, Infrastructure, Soft-AP
	Wi-Fi Security	WPA-PSK / WPA2-PSK, WPA-Enterprise (TTLS/PEAP)
	Web Applications	WebSerialMonitor, WebRemoteControl (Push/Slide)IPv4/IPv6 Dual Stack
Software	Network Protocols	TCP/UDPICMP, DHCP, HTTP, Telnet, SSH, SMTP, ESMTMP, DNS
	Security	SSL/TLS
	Network Configuration	Via Web

Figure 2 shows a smartphone application; the main function is to show the Charging Controller and Monitoring interface. Figure 2a shows the Charging Controller, where the user can select between Auto Control Mode and User Control Mode. The charging current is automatically determined by considering the temperature of the Auto Control Mode. Auto Control Mode determines the control current in real-time according to the temperature state and charges it. In the case of rapid charging, by applying a large current to the battery, it is charged faster than normal charging. Therefore, rapid charging may cause problems of temperature rise of the battery and fire. In the case of the proposed Auto Control Mode, it is charged to determine the reference value of the current according to the temperature state. There is an advantage in that the battery can be safely charged by considering the temperature state.

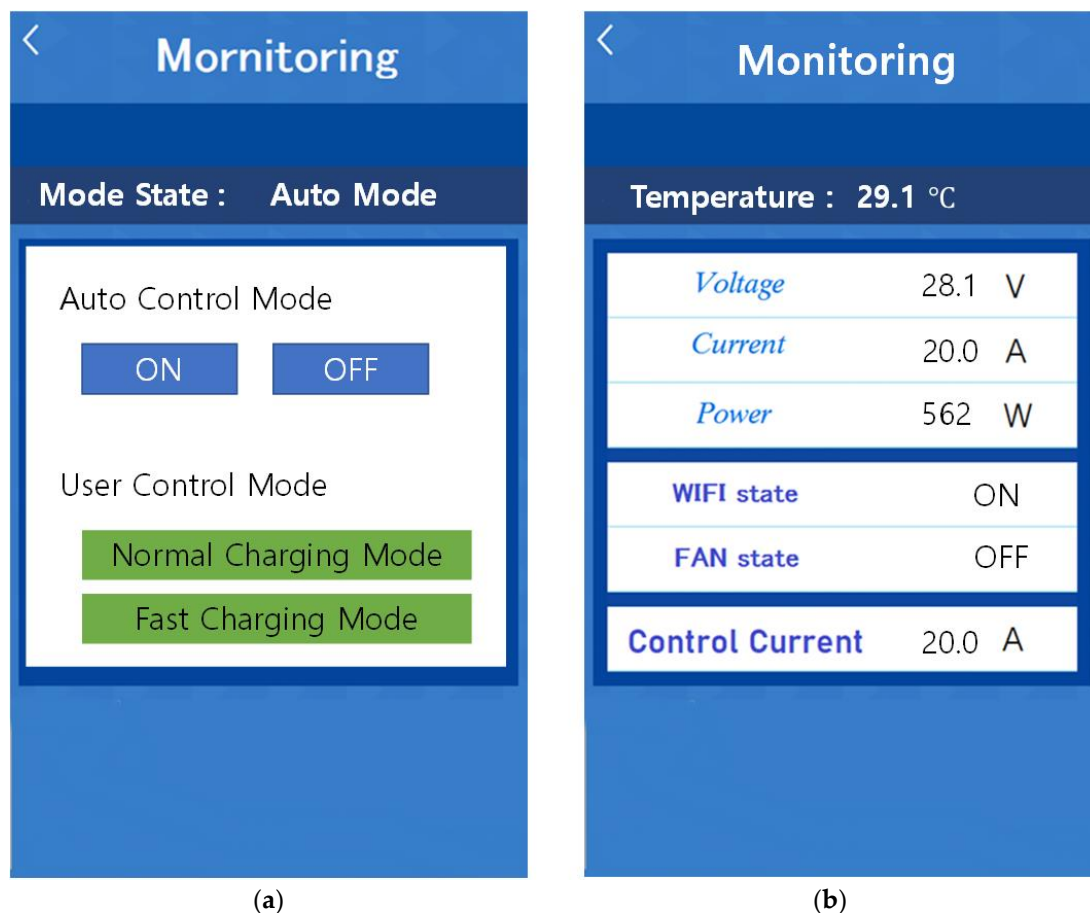


**Figure 2.** Smartphone application interface: (a) First interface; (b) Second interface.

Figure 2b shows the Monitoring interface; voltage, current, power, Wi-Fi connection status, cooling fan operating status, and control current values are displayed on the display. In this part, the user can easily check the current charging status. By checking the current being controlled and the charging current, the current state of charge can also be identified; moreover, the user can also check the current temperature and Wi-Fi connection status.

## 2.2. LLC Resonant Converter

High efficiency, high power density, and power are the major driving force for DC/DC converter applications. The DC/DC converter with high switching frequency and high efficiency is highly demanded. LLC resonant converters can use Zero Voltage Switching technology to minimize switching losses, and in addition, it can minimize the switching loss compared to the PWM (Pulse Width Modulation) type converter and operates at a higher switching frequency. High circulating energy and high switching losses occur when

operating at high input conditions; however, it is not suitable for general DC/DC converter applications. LLC resonant converters have two resonant frequencies; in this case,  $L_r$  and  $C_r$  determine the higher resonant frequency, while the low resonant frequency is determined by the series inductances of  $L_m$  and  $L_r$ . In the case of a high resonant frequency region, it can operate in the ZVS region. Therefore, it can be designed to operate in the ZVS region. The benefit of LLC resonant converter is narrow switching frequency range at light load and ZVS operation at no load [18,19]. Figure 3 shows the LLC resonant tank; the LLC resonant tank has a structure in which  $C_r$  and  $L_r$  are connected in series, and  $L_m$  is connected in parallel [20,21]. The resonant converter can be divided into series resonant converter, parallel resonant converter, and LCC resonant converter according to the combination of capacitor and inductor. Each converter has a different resonance frequency and voltage gain, depending on the coupling state of the resonance tank. When the resonant inductor and the capacitor are of the series-parallel (LCC) type, there is a disadvantage that a filter inductor must be configured on the output side. The series resonant converter is a type in which a resonant inductor and a resonant capacitor are connected in series and has low efficiency. The parallel resonant converter is a type in which a resonant inductor and a resonant capacitor are connected in parallel and has a disadvantage in that a filter reactor must be configured on the output side [22,23].

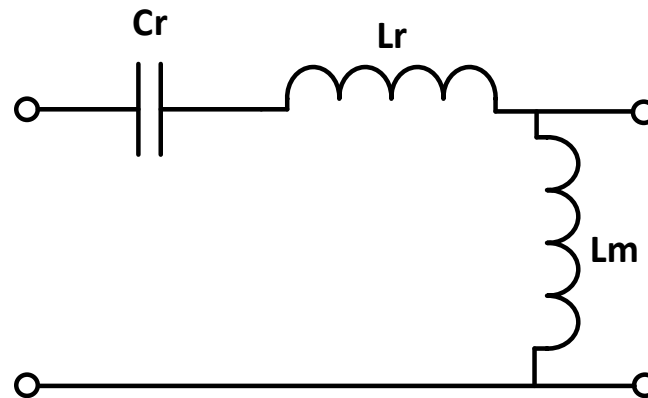


Figure 3. LLC Resonant tank.

#### LLC Resonant Converter Operation

The voltage gain characteristic of the LLC resonant converter can be divided into ZVS and ZCS regions as shown in Figure 1. A resonant converter has two resonant frequencies; one is determined by  $L_r$  and  $C_r$ , and the other is determined by  $L_m$ ,  $C_r$ , and load conditions. When the load becomes heavy, the resonant frequency operates at a higher frequency. The gain of the resonant converter is determined through the transformer ratio and the resonant tank gain. The voltage gain of the resonant tank is determined through Equation (1).

$$\left| \frac{V_o(s)}{V_{in}(s)} \right| = \frac{F_1^2(m-1)}{\sqrt{(m \cdot F_1^2 - 1)^2 + F_1^2 \cdot (F_1^2 - 1)^2 \cdot (m-1)^2 \cdot Q^2}} \quad (1)$$

where the values of quality factor ( $Q$ ), normalized switching frequency ( $F_1$ ) and  $m$  can be defined as in Equations (2)–(4) where  $f_s$  is switching frequency.

$$Q = \frac{\sqrt{L_r/C_r}}{R_{ac}} \quad (2)$$

$$m = \frac{L_r + L_m}{L_r} \quad (3)$$

$$F_1 = \frac{f_s}{f_r} \quad (4)$$

The resonant frequency can be expressed by Equation (5).

$$f_r = \frac{1}{2\pi\sqrt{L_r \cdot C_r}} \tag{5}$$

The voltage gain curve of the resonant tank can be expressed based on Equation (1). The voltage gain curve is determined by the values of  $Q$  and  $m$ ;  $Q$  factor is affected by load conditions. A high value of  $Q$  means a heavy load [24,25]; when the  $Q$  value is low, it means a light load. For fast charging, a high current control value is required. Therefore, the value of the voltage gain operates in the range of 0.7–1.4. The value of  $Q$  is selected as 0.4. The graph of voltage gain varies according to the value of  $Q$ . The next step is to choose a value for  $m$ . When the value of  $m$  is low, it has a high voltage gain, and a narrow frequency range and flexible adjustment are possible. A high value of  $m$  has a high magnetizing inductance and a low magnetizing circulating current. Therefore, in order to obtain high efficiency, the value of  $m$  should be selected between 6 and 10, where, the values of  $Q$  and  $m$  are selected as 0.4 and 7.6. Resonant inductor  $L_r$  is 0.18mH, resonant inductor  $L_m$  is 1.2mH and  $C_r$  is 0.1 uF.

The voltage curve graph can be expressed through Figure 4. Additionally, the graph is drawn by MATLAB, version 2017 (MathWorks, Boston, MA, USA). It can be seen from the voltage gain curve that a boundary exists between the inductive impedance and capacitive impedance. Therefore, the inductive and capacitive operating area can be divided into ZVS and ZCS region. The purpose of defining the two domains is an inductive operation over the entire input voltage and load current range. ZVS operation takes place in the inductive region. Moreover, in capacitive operation, the current leads the voltage. In the switching operation of MOSFET, when the switch is turned off, a reverse current flow through the body diode of the MOSFET. The current flows through the body diode to perform hard switching. In addition, reverse recovery losses and noise may occur as the other MOSFET turn on, resulting in high current [26–28].

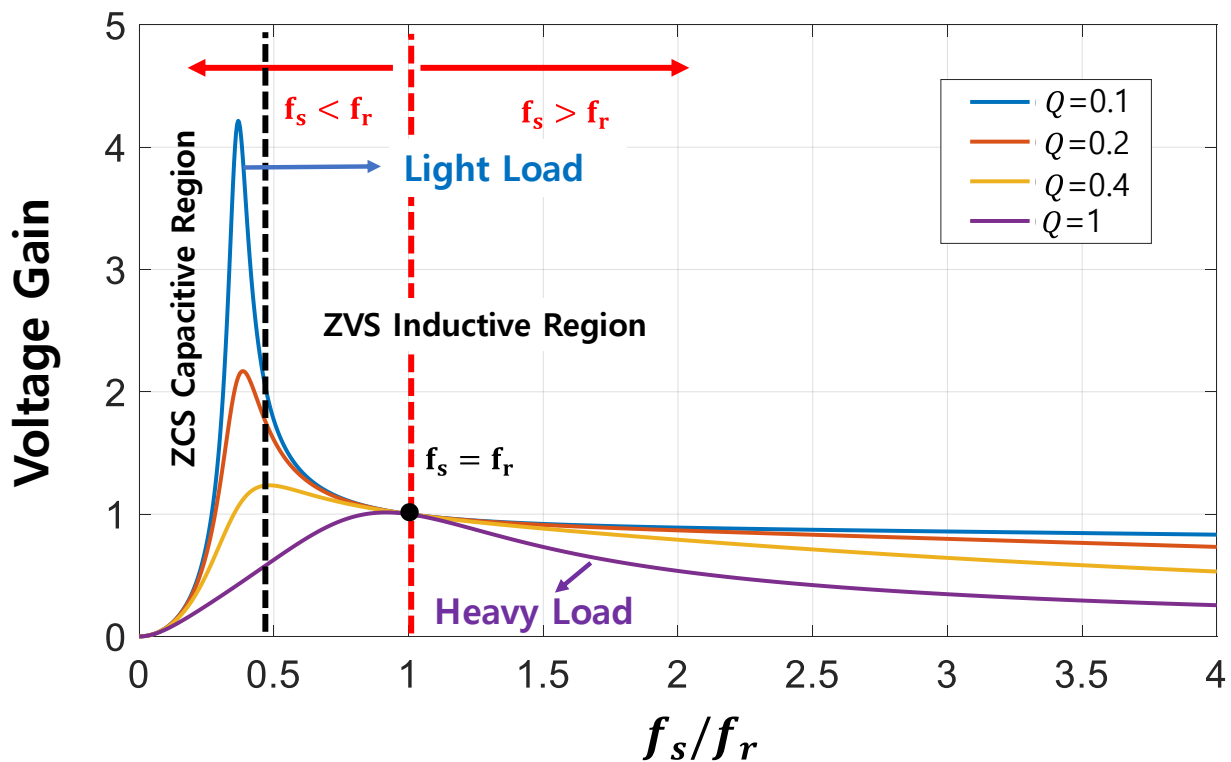
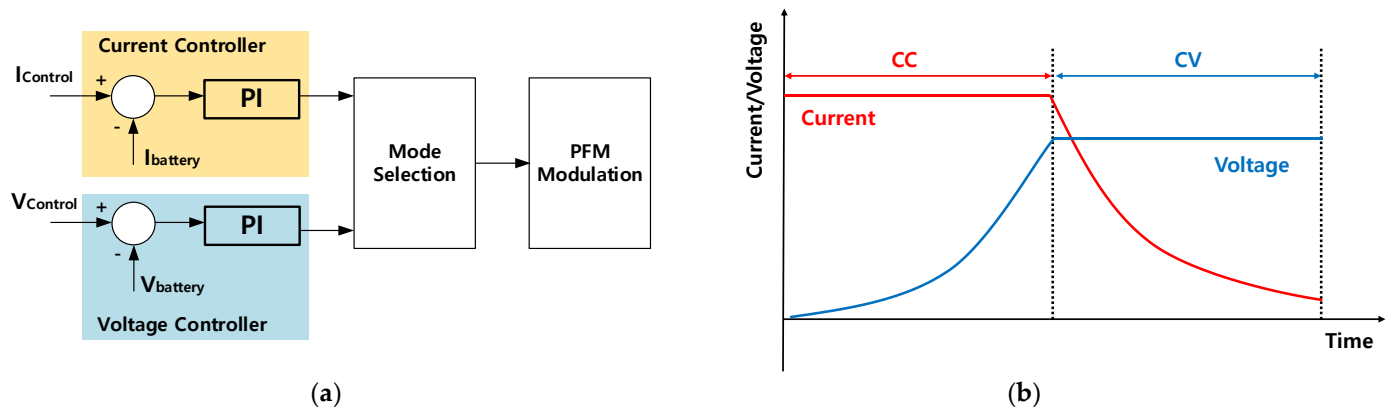


Figure 4. Voltage gain curve.

### 3. Proposed Controller Structure

This section shows the proposed controller block diagram and the flowchart of the IoT-based controller. The CC/CV charging method is a widely used method for charging lead-acid batteries and lithium-ion batteries. The CC (Constant Current) method is a method of charging with a current with a constant control value. The CV (Constant Voltage) method is a charging method based on a voltage of a constant control value. Figure 5a shows the control block diagram of CC/CV charging method. The two charging methods are the method of controlling the current and voltage through PFM control through the PI controller according to the reference value. A PFM signal is applied to the switching element of the LLC resonant converter, and the desired output is obtained through a switching operation accordingly. Figure 5b shows the voltage/current charging graph; when the battery starts charging, it is initially charged with a constant control current through the CC method. As charging proceeds, the voltage gradually rises. When the voltage rises to the set value, from then on, it charges in CV mode. In the constant voltage state, the value of the current gradually decreases, and charging is complete when the current decreases to near zero. The CC/CV charging method, as shown in Figure 5b, is the most widely used charging method. In addition to the CC/CV charging method, there are the CC charging method and the CV charging method; however, in the CC charging method, the voltage of the closed-circuit due to the internal resistance of the cell becomes higher than the voltage of the device itself, and thus 100% charging is not possible. In the CV charging method, an overcurrent may occur due to the potential difference in the initial voltage.



**Figure 5.** Charging Algorithm: (a) Control structure during charging mode; (b) CC–CV curve.

The main control goal of the proposed ICT system is to allow the user to check the charging status and select between quick charging and normal charging mode. The charging level is directly related to the charging rate. If the user, that is, the consumer side management is considered, the user's desired charging can be considered; indeed, charge level or speed has a direct correlation with battery life. In addition, you can check the charging status of the charger in real-time through the smartphone application. The operational flowchart of the IoT system is shown in Figure 6.

The operation of the proposed system starts with the operation of the IoT system and the charging system. In the initial start, the charger and IoT system are operated. After operation, the IoT system creates a web server and uploads data to the web. The smartphone app accesses the web server and reads data. Check the operation and connection status of the IoT system, smartphone app, and charger. If all the system states are not satisfied, the initial operation is restarted. When the operation and connection status of all systems are satisfied, the charging mode is selected through the smartphone app. Charging does not start until the mode is selected, but waits for the mode to be selected. When the charging mode is selected, the connection status of the battery and the readiness for charging are checked through the data of the output voltage and input voltage. If the output and input

voltages are not met, the operation is terminated. When the values of the output and input are met, the soft-start starts charging. Once charging starts, the charging status is transmitted to the web server, and the user can check the data. Charging is repeated until it reaches 33.6V, and data are sent to the web server in real-time. When 33.6V is met, charging is terminated. When charging is finished, the Mode State of the first interface of the app is displayed as Finish.

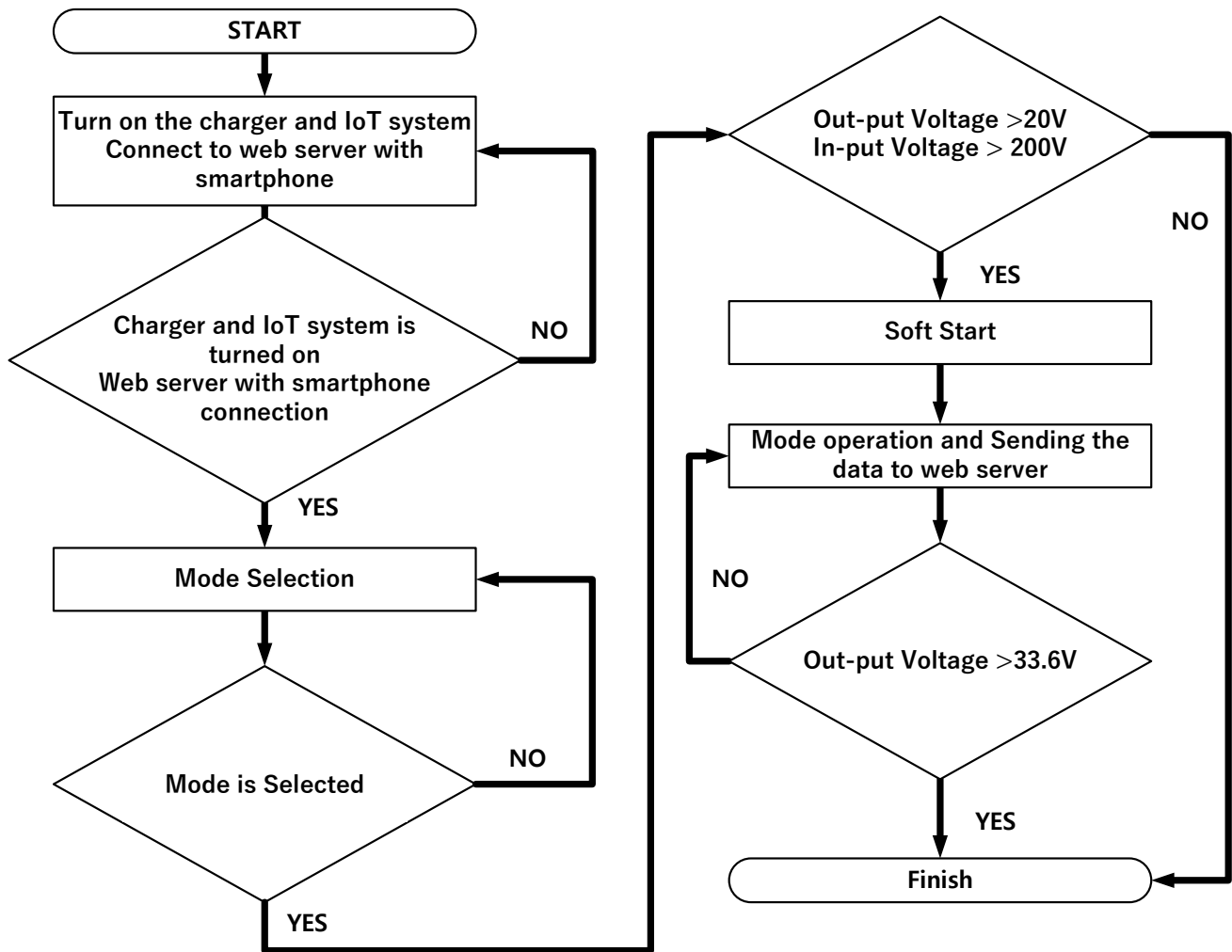


Figure 6. Flow chart of the IoT controller.

In general, the allowable charging temperature of lithium-ion batteries is between 20 and 40 degrees. In addition, the temperature at which rapid charging is possible is 25 to 30 degrees Celsius, so that rapid charging is possible; however, in the case of rapid charging, it is a charging method that affects the lifespan of the battery and the temperature rise. Therefore, appropriate charge control is required to mitigate the battery life and temperature rise. In this paper, we propose a charging method that automatically controls the charging current of the battery according to the temperature using the Auto mode. A method for a user to charge the battery is divided into a user charging mode and an Auto mode. Users can select a charging method and check the charging status in real-time; in the user charging mode, the user selects and charges a fixed control current in a general charging method. On the other hand, in the case of Auto mode, it is a charging method by calculating an appropriate control current based on real-time temperature information; by increasing or decreasing the control current based on the temperature information, it reduces the temperature rise and burden on the battery during charging. Figure 7a,b

shows graphs showing the charging current according to temperature; the two graphs can be expressed as Equations (6) and (7). Figure 7a,b graphs are divided based on the battery temperature of 30 degrees. Due to the nature of the battery, the performance varies depending on the temperature. Therefore, the current was determined considering the low and high-temperature conditions. A general charging system is charged in the CC mode through a constant reference current value without considering the temperature state; however, in the proposed method, the charging parameters change in real-time according to the temperature state.

$$\text{(When, } 31 \sim 40 \text{ }^\circ\text{C)} \text{ Reference Current} = -2 * \text{Temperature value} + 90 \quad (6)$$

$$\text{(When, } 20 \sim 30 \text{ }^\circ\text{C)} \text{ Reference Current} = 2 * \text{Temperature value} - 30 \quad (7)$$

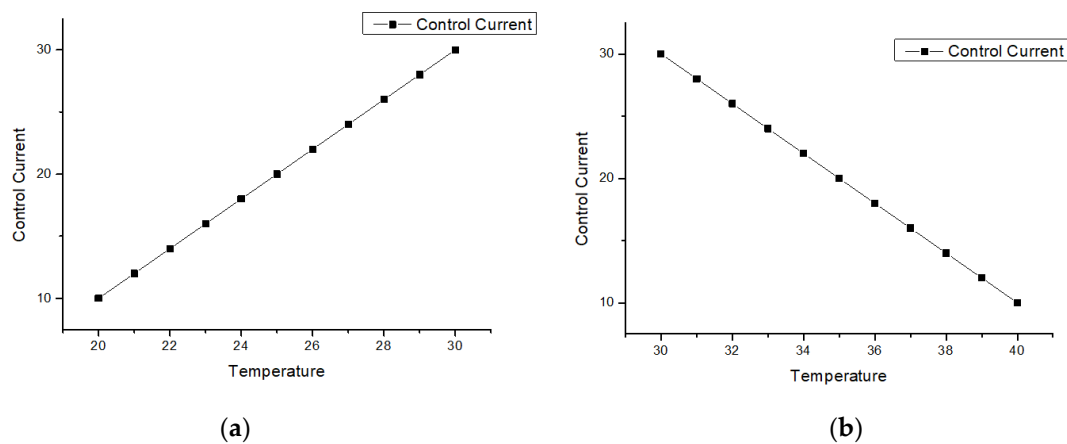


**Figure 7.** Charging Algorithm: (a) Control structure during charging mode; (b) CC-CV curve.

#### 4. Results and Discussion

Figure 8 shows the experimental setup of the proposed charger system. It consists of an LLC resonant converter, IoT system and Li-ion Battery. Figure 9 shows the charging waveform of the LLC converter. Charging shows the waveform in Fast Charging mode. it is controlled in CC mode. also, it shows the operation in the ZVS region through the waveform of the inductor and the waveform of the primary side voltage in the charging waveform. The frequency is modulated to follow the current value selected as the control value. In Fast Charging mode, it operates at the same frequency as the resonant frequency and converts power to the most efficient state. However, when fast charging is performed for a long period of time, the temperature of the battery and converter may rise, which may decrease the efficiency and safety of the battery. Therefore, the proposed method provides the user to select the filling level. Also, in the case of Auto mode, it is controlled in consideration of the temperature condition of the battery.

Figure 10 shows the operation waveform and the monitoring interface in the proposed Auto mode. In the case of Auto mode, the control current is determined according to the temperature. Figure 10 shows the time of operation at a relatively high temperature; The control current is determined and operated according to the temperature, and it can be confirmed that the voltage gain is changed by changing the Fast Charging mode and the switching frequency by changing the control current command, thereby controlling the charging current. Moreover, it shows the operation in the ZVS region through the waveform of the inductor and the waveform of the primary side voltage in the charging waveform. Through the interface, the user can easily know the current battery voltage, charging current, temperature and power status.

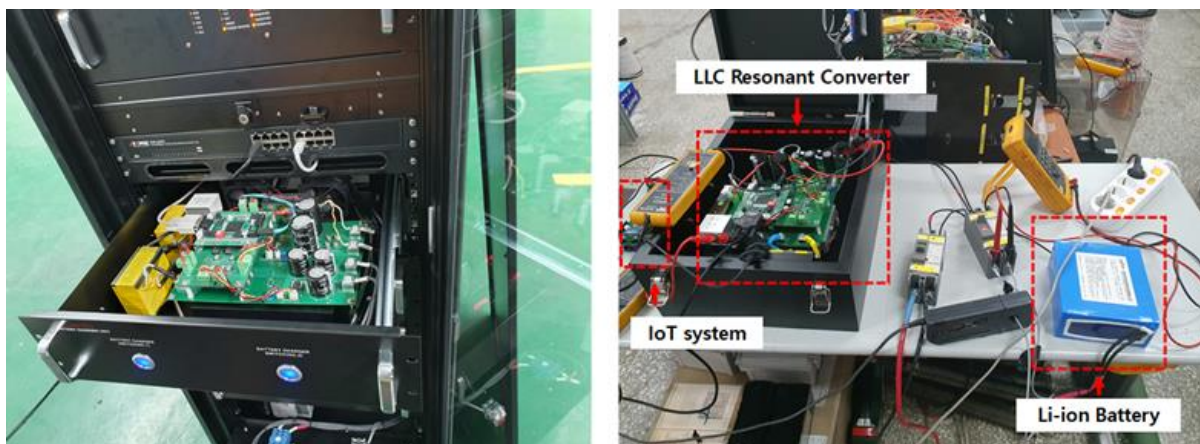
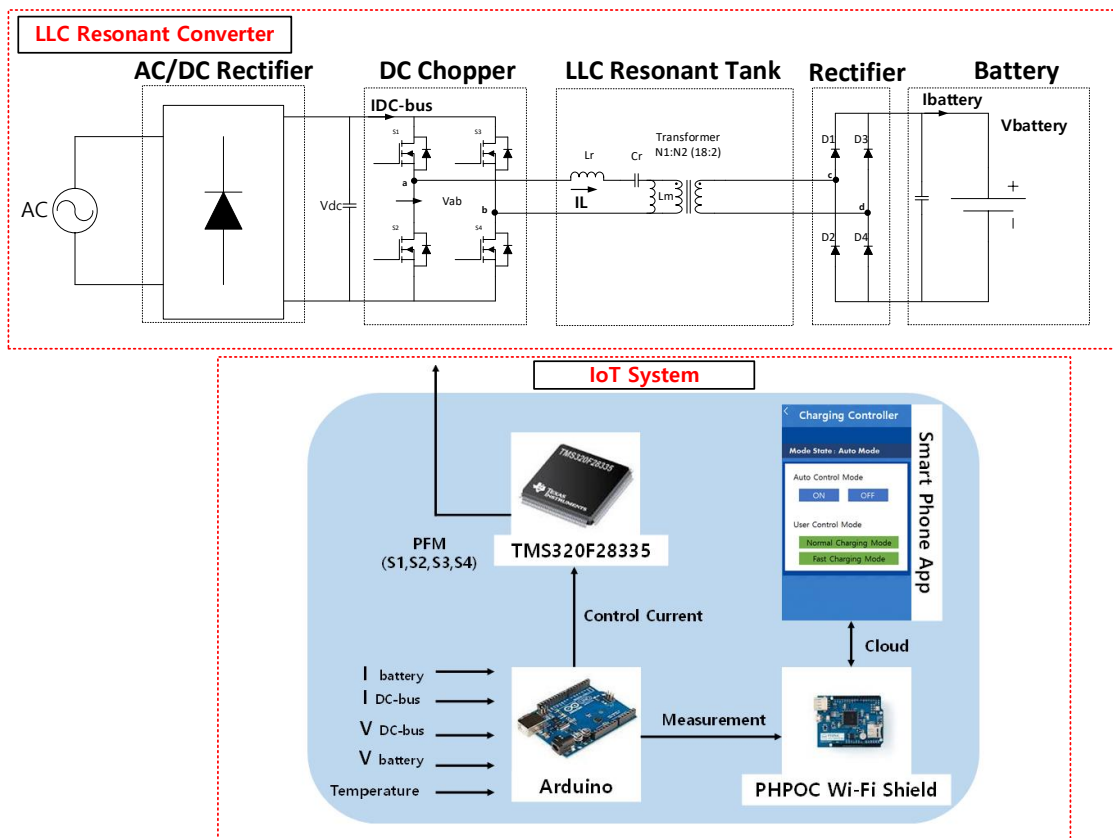
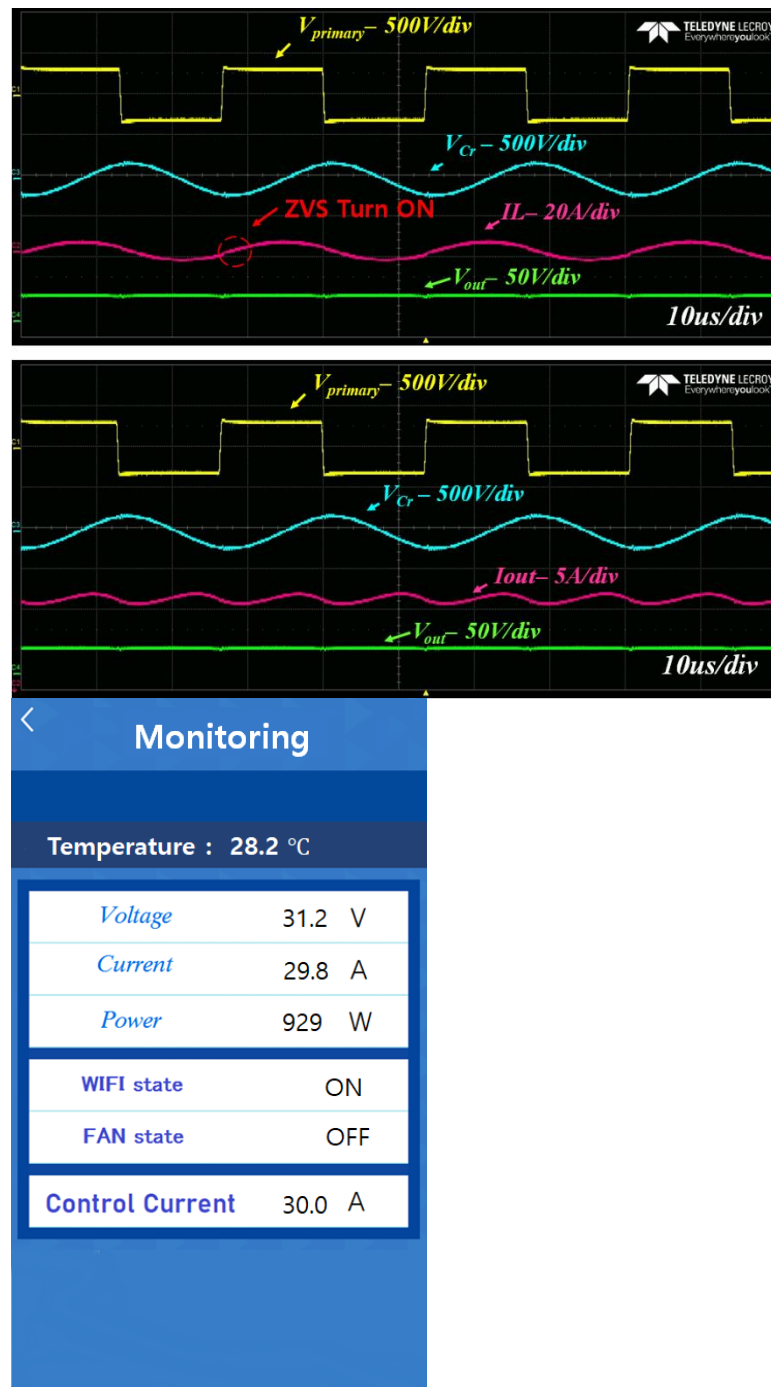


Figure 8. The prototype of the proposed system.

Figure 11 shows the operating point at a relatively low temperature. In Auto mode, the control current is determined according to the temperature, while the monitoring interface in the figure shows the situation when the charging voltage and temperature are low. In Auto mode, the control charging current is controlled to 30A or less; in addition, switching loss can be minimized by ZVS operation, and in the case of Auto mode, it is decided based on the graph of the current command according to the temperature in Section 5. In Auto mode, the temperature rises, and safe charging of the battery and converter is possible compared to the general charging method; it reduces the burden on the battery by rationally giving the charge current command according to the situation, notifying the user of the state of the battery in real-time, and the user can decide how to charge the battery so that the battery can be managed efficiently.



**Figure 9.** Charging wave form and corresponding smartphone application screen snapshots (Fast Charging mode, Temperature = 29.1 °C).

Figure 9 shows the operation in the Fast Charging Mode selected by the user. Moreover, Figures 10 and 11 show the waveform in Auto mode. In Fast Charging Mode, it is shown that it operates without considering the temperature. If the temperature is 28.2 °C, we have a control command of about 26.4 A, depending on the calculation. It can be seen that the Fast Charging Mode is fixed and controlled with a control current of 30 A. Unlike Figures 10 and 11, it has a fixed current control value, so the charging level is high; however, if temperature is not taken into account, it may cause battery life or excessive temperature rise, which may cause a fire. Figures 10 and 11 operate in Auto mode while Figure 10 shows the Auto mode above 31 °C. The control current value is calculated and controlled

by Equation (6). In Figure 11, the control current value is calculated by Equation (7). Figure 9 has a constant current reference. On the other hand, Figures 10 and 11 have the control current command is calculated in real-time. Therefore, compared to the Fast Charging Mode, it is advantageous for the temperature rise of the battery and battery life by compensating for the temperature; however, there is a disadvantage that the charging speed is slow compared to the Fast Charging Mode.

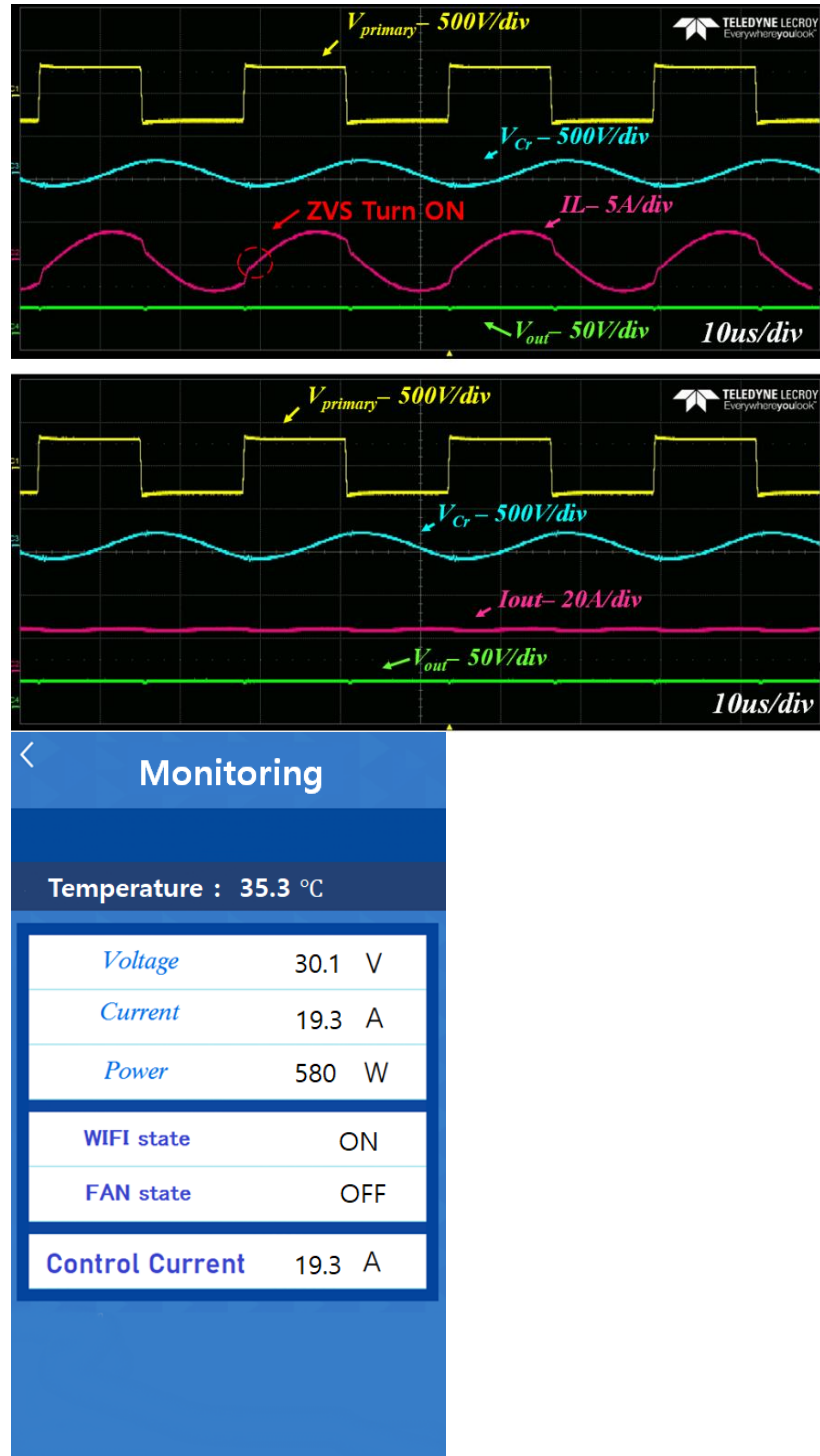
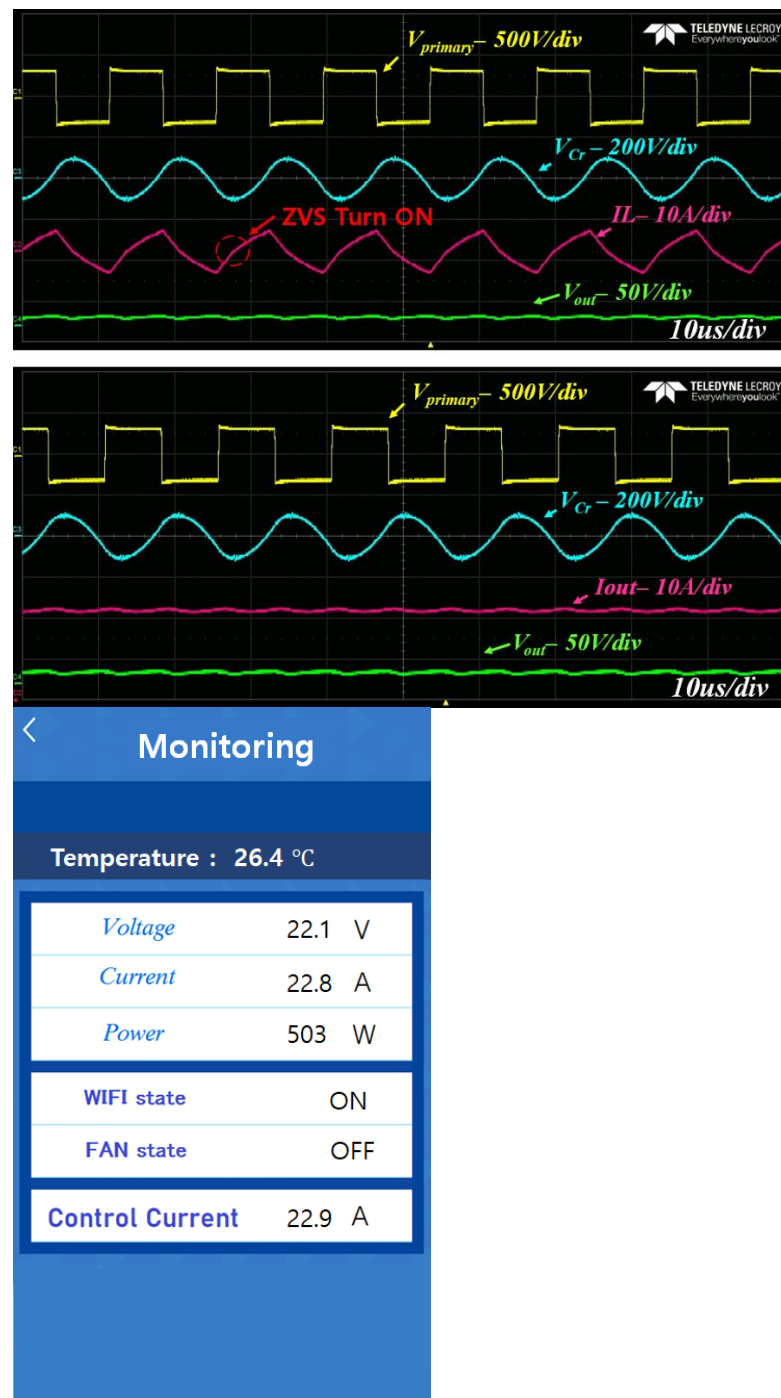


Figure 10. Charging wave form and corresponding smartphone application screen snapshots (Auto mode, Temperature = 35.3 °C).



**Figure 11.** Charging wave form and corresponding smartphone application screen snapshots (Auto mode, Temperature = 26.4 °C).

Various studies are being conducted to determine the fire or lifecycle of batteries. In particular, in the case of fast charging, it can be charged in a shorter time compared to a general charging method; however, rapid charging causes the battery temperature to rise. The temperature rise of the battery affects the lifecycle and performance of the battery. The change in the charging current according to the temperature suggested in this paper reduces the strain on the battery by lowering the charging current when the temperature rises. The control of the charging current according to the temperature of the battery was checked for a battery with a low capacity. In the future, it is necessary to verify the experiment on high-capacity batteries.

## 5. Conclusions and Future Work

In this paper, a charger applied with IoT-based real-time monitoring and a charging method considering the temperature state is proposed. In the case of a general charger, there is a restriction in the user's ability to check or control the charging state and charging method. In this paper, the user can easily check the charging status in real-time. In addition, it has been proposed that the user can select a charging method as well. As for the charging method, the user can select a general charging method and a charging method in consideration of temperature. The charging method considering the temperature is designed to safely and quickly charge the battery by controlling the charging level according to the temperature of the battery. Experiments were conducted by manufacturing a charger and IoT system prototype. The proposed prototype calculates the control current according to the temperature situation. It has been shown that the charger can be controlled based on the calculated control current. Based on the experimental results, it was shown that the switching loss can be reduced, and safe charging can be controlled through ZVS operation during charging. The system presented in this paper was verified through experiments and prototype systems using small-capacity batteries, such as LEVs. Future research and verification through high-capacity batteries such as EVs and ESSs are needed. The battery market is growing day by day, and battery management is becoming more important. We propose a battery management system considering only the battery temperature. In the case of a battery, it is also greatly affected by the ambient temperature. In the future, a battery management system that considers the temperature of the battery and the ambient temperature is required. We plan to design and manufacture a real-time management algorithm that takes into account verification in high-capacity batteries and ambient temperature.

**Author Contributions:** K.P, H.-J.K. and D.-H.K. conceptualized the idea of this research project; D.-H.K., M.-S.K. discussed the Efficient management of fast charging system based on real-time monitoring system; the proposed algorithm and controlled were designed by M.-S.K., D.-H.K., H.-J.K.; the power conversion PCB board was designed by H.-J.K.; the fabrication and experimental setup were mostly carried out by D.-H.K. under the supervision of K.P. and H.-J.K.; the paper was written by D.-H.K., K.P. and H.-J.K. All authors have read and agreed to the published version of the manuscript.

**Funding:** This research received no external funding.

**Institutional Review Board Statement:** Not applicable.

**Informed Consent Statement:** Not applicable.

**Data Availability Statement:** Not applicable.

**Conflicts of Interest:** The authors declare no conflict of interest.

## References

1. Fu, Y.; Jia, C.; Huang, Y.; Ren, W. Influence of electric vehicles on reliability of power system containing wind power. In Proceedings of the 2017 IEEE Transportation Electrification Conference and Expo, Asia-Pacific (ITEC Asia-Pacific), Harbin, China, 7–10 August 2017; pp. 1–5.
2. Alshahrani, S.; Khalid, M.; Almuahini, M. Electric vehicles beyond energy storage and modern power networks: Challenges and applications. *IEEE Access* **2019**, *7*, 99031–99064. [[CrossRef](#)]
3. Kwak, B.; Kim, M.; Kim, J. Add-On Type Pulse Charger for Quick Charging Li-Ion Batteries. *Electronics* **2020**, *9*, 227. [[CrossRef](#)]
4. Dimitrov, B.; Hayatleh, K.; Barker, S.; Collier, G.; Sharkh, S.; Cruden, A. A Buck-Boost Transformer less DC–DC Converter Based on IGBT Modules for Fast Charge of Electric Vehicles. *Electronics* **2020**, *9*, 397. [[CrossRef](#)]
5. Brzezinska, D.; Bryant, P. Performance-Based Analysis in Evaluation of Safety in Car Parks under Electric Vehicle Fire Conditions. *Energies* **2022**, *15*, 649. [[CrossRef](#)]
6. Zeng, J.; Zhang, G.; Yu, S.S.; Zhang, B.; Zhang, Y. LLC resonant converter topologies and industrial applications—A review. *Chin. J. Electr. Eng.* **2020**, *6*, 73–84. [[CrossRef](#)]
7. Shen, Y.; Zhao, W.; Chen, Z.; Cai, C. Full-bridge LLC Resonant Converter with Series-parallel Connected Transformers for Electric Vehicle On-board Charger. *IEEE Access* **2018**, *6*, 13490–13500. [[CrossRef](#)]
8. Moreno, M.; Pereda, J.; Rojas, F.; Dominguez-Lopez, I. Decoupled PI Controllers Based on Pulse-Frequency Modulation for Current Sharing in Multi-Phase LLC Resonant Converters. *IEEE Access* **2021**, *9*, 15283–15294. [[CrossRef](#)]

9. Ta, L.A.D.; Dao, N.D.; Lee, D.-C. High-Efficiency Hybrid LLC Resonant Converter for On-Board Chargers of Plug-In Electric Vehicles. *IEEE Trans. Power Electron.* **2020**, *35*, 8324–8334. [[CrossRef](#)]
10. Vu, H.; Choi, W. A Novel Dual Full-Bridge LLC Resonant Converter for CC and CV Charges of Batteries for Electric Vehicles. *IEEE Trans. Ind. Electron.* **2017**, *65*, 2212–2225. [[CrossRef](#)]
11. Li, D.; Yang, Q.; An, D.; Yu, W.; Yang, X.; Fu, X. On location privacy preserving online double auction for electric vehicles in microgrids. *IEEE Internet Things J.* **2019**, *6*, 5902–5915. [[CrossRef](#)]
12. Xu, L.; Mcardle, G. Internet of too many things in smart transport: The problem, the side effects and the solution. *IEEE Access* **2018**, *6*, 62840–62848. [[CrossRef](#)]
13. Metwly, M.Y.; Abdel-Majeed, M.S.; Abdel-Khalik, A.S.; Torki, M.; Hamdy, R.A.; Hamad, M.S.; Ahmed, S. IoT-Based Supervisory Control of an Asymmetrical Nine-Phase Integrated on-Board EV Battery Charger. *IEEE Access* **2020**, *8*, 62619–62631. [[CrossRef](#)]
14. Shen, Y.; Zhao, W.; Chen, Z.; Cai, C. Full-Bridge LLC Resonant Converter with Series-Parallel Connected Transformers for Electric Vehicle On-Board Charger. *IEEE Access* **2018**, *6*, 13490–13500. [[CrossRef](#)]
15. Kim, D.-H.; Kim, M.-S.; Hussain Nengroo, S.; Kim, C.-H.; Kim, H.-J. LLC Resonant Converter for LEV (Light Electric Vehicle) Fast Chargers. *Electronics* **2019**, *8*, 362. [[CrossRef](#)]
16. Arduino Uno REV3. Available online: <https://www.amazon.com/Arduino-A000066-ARDUINO-UNO-R3/dp/B008GRTSV6/> (accessed on 1 February 2022).
17. PHPOC Wi-Fi Shield. Available online: [https://www.phpoc.com/phpoc\\_wifi\\_shield\\_R1.php](https://www.phpoc.com/phpoc_wifi_shield_R1.php) (accessed on 1 February 2022).
18. Shah, S.S.; Rastogi, S.K.; Bhattacharya, S. Paralleling of LLC Resonant Converters. *IEEE Trans. Power Electron.* **2021**, *36*, 6276–6287. [[CrossRef](#)]
19. Yeon, C.; Kim, J.; Park, M.; Lee, I.; Moon, G. Improving the Light-Load Regulation Capability of LLC Series Resonant Converter Using Impedance Analysis. *IEEE Trans. Power Electron.* **2017**, *32*, 7056–7067. [[CrossRef](#)]
20. Wei, Y.; Luo, Q.; Mantooth, A. Comprehensive analysis and design of LLC resonant converter with magnetic control. *CPSS Trans. Power Electron. Appl.* **2019**, *4*, 265–275. [[CrossRef](#)]
21. Tang, Y.; Kong, D.; Duan, C.; Sun, H. Optimal Design of LLC Resonant DC Transformer under Adaptive Frequency Tracking Strategy. *Electronics* **2020**, *9*, 2160. [[CrossRef](#)]
22. Wei, Y.; Luo, Q.; Mantooth, H.A. An LLC and LCL-T resonant tanks based topology for battery charger application. *CPSS Trans. Power Electron. Appl.* **2021**, *6*, 263–275. [[CrossRef](#)]
23. Reddy, V.B.; Harischandrapa, N. Comparison of Phase-Shift and Modified Gating Schemes on Working of DC-DC LCL-T Resonant Power Converter. *IEEE Trans. Circuits Syst. II Express Briefs* **2021**, *68*, 346–350. [[CrossRef](#)]
24. Lee, I.; Moon, G. The  $s$ - $Q$  Analysis for an LLC Series Resonant Converter. *IEEE Trans. Power Electron.* **2014**, *29*, 13–16. [[CrossRef](#)]
25. Li, Y.; Shao, S.; Chen, H.; Zhang, J.; Sheng, K. High-gain high-efficiency IPOS LLC converter with coupled transformer and current sharing capability. *CPSS Trans. Power Electron. Appl.* **2020**, *5*, 63–73. [[CrossRef](#)]
26. Fei, C.; Lee, F.C.; Li, Q. High-Efficiency High-Power-Density LLC Converter with an Integrated Planar Matrix Transformer for High-Output Current Applications. *IEEE Trans. Ind. Electron.* **2017**, *64*, 9072–9082. [[CrossRef](#)]
27. Shah, S.S.; Iyer, V.M.; Bhattacharya, S. Exact Solution of ZVS Boundaries and AC-Port Currents in Dual Active Bridge Type DC-DC Converters. *IEEE Trans. Power Electron.* **2019**, *34*, 5043–5047. [[CrossRef](#)]
28. Kundu, U.; Yenduri, K.; Sensarma, P. Accurate ZVS Analysis for Magnetic Design and Efficiency Improvement of Full-Bridge LLC Resonant Converter. *IEEE Trans. Power Electron.* **2017**, *32*, 1703–1706. [[CrossRef](#)]